Supporting Information

Lithium bis(trifluoromethanesulfonyl)imide Assisted Dual-Functional Separator Coating Materials Based on Covalent Organic Framework for High-Performance Lithium-Selenium Sulfide Battery

Yan Yang[‡a], Xu-Jia Hong[‡a], Chun-Lei Song[a], Guo-Hui Li[a], Yi-Xin Zheng[a], Dan-Dan Zhou[a], Min Zhang[b], Yue-Peng Cai*[a] and Hongxia Wang*[c]

[a]*School of Chemistry and Environment, Guangzhou Key Laboratory of Materials for Energy Conversion and Storage, Guangdong Provincial Engineering Technology Research Center for Materials for Energy Conversion and Storage, South China Normal University Guangzhou, 510006, P. R. China*

[b]*School of Materials Science and Energy Engineering, Foshan University, Foshan, 528000, P. R. China.*

[c]*School of Chemistry, Physics and Mechanical Engineering, Queensland University of Technology(QUT), Brisbane, QLD 4001, Australia*

‡*These authors have contributed equally.*

Table S1. Performance comparison of the Li-SeS_2 batteries.

Electorde Materials	Separator	The mass fraction of SeS_2 (wt%)	Areal SeS_2 mass loading (mg cm^{-2})	Current Density (A/g)	Cycle number	Specific Capacity (mAh/g)	Specific Capacity (mAh/cm^2)	voltage range(V)	Refs.
CoS_2@LRC/SeS_2	Celgard	70	2.3-2.5	0.5	400	470	1.08-1.18	1.8-2.8	1
CMK-3/SeS_2@PDA	Celgard	70	2.6–3.0	2	500	350	0.91-1.05	1.6–2.8	2
Co-N-C/SeS_2	Celgard	66.5	3.2	0.27	200	970.2	3.10	0.8-3.0	3
SeS_2 /DLHC	-	75	0.8-1.0	0.2	100	~910	~0.73-0.91	1.0-3.0	4
SeS_2 /HMCNCs	-	78.1	1.2–1.5	0.2	100	812.6	0.98-1.22	1.0-3.0	5
HMC@TiN/SeS_2	Celgard	70	1.0	0.22	100	690	0.69	1.8-2.8	6
SeS_2 @MCA	Celgard	49.3	1.5-2.0	0.2	130	308	0.31-0.42	0.8-4.0	7
S–SeS_2–DIB@ KB600	Celgard	<70	<0.8	1	500	~600	<0.48	1.8-2.8	8
pPAN/SeS_2	Celgard	63	1.26	4	2000	633	0.80	1.0-3.0	9
SeS_2/super-P	**COFs/Celgard**	**80**	**2.0**	**0.56**	**200**	**678.8**	**1.357**	**1.7-2.7**	**This work**
SeS_2/MWCNT	**COFs/Celgard**	**80**	**4.0**	**1.12**	**800**	**416.3**	**1.665**		

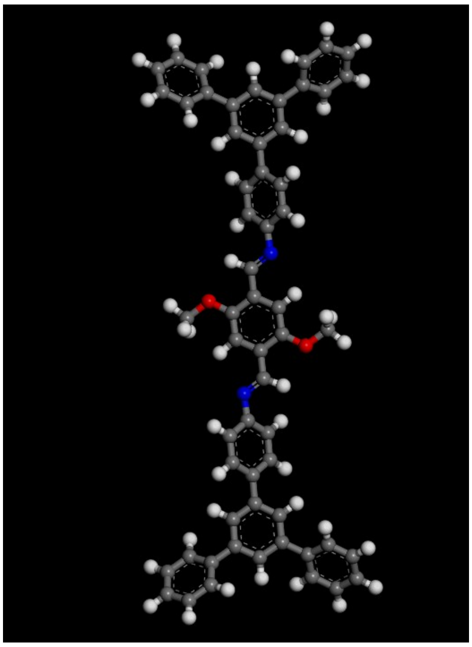

Figure S1. The segment of TPB-DMTP-COF for modelling its interaction with different species in the electrolyte

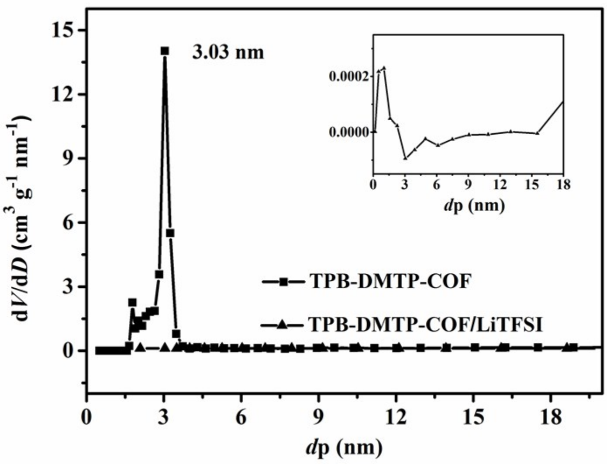

Figure S2. Pore size distribution of TPB-DMTP-COF and TPB-DMTP-COF/LiTFSI (The inset figure is the pore size distribution of TPB-DMTP-COF/LiTFSI).

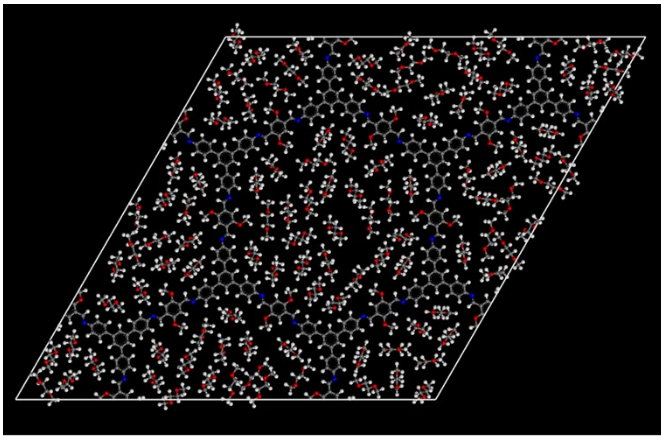

Figure S3. The DFT calculation of binding sites between TPB-DMTP-COF and DME.

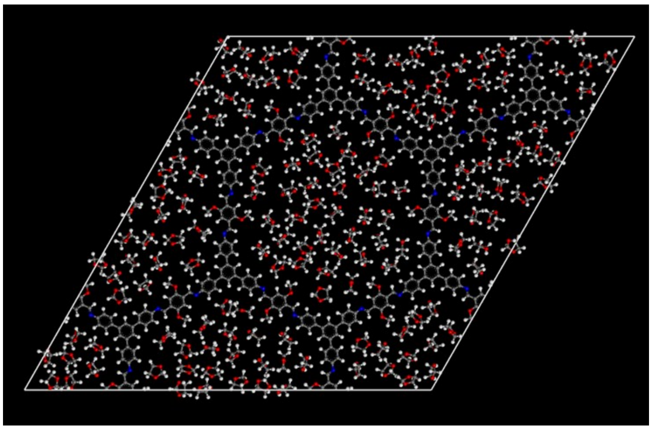

Figure S4. The DFT calculation of binding sites between TPB-DMTP-COF and DOL.

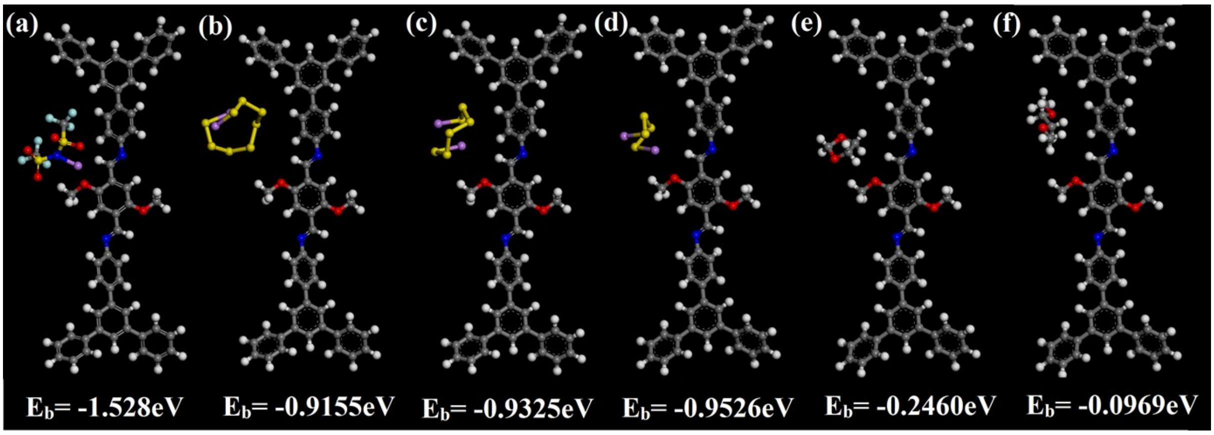

Figure S5. The interaction fragment between TPB-DMTP-COF and (a) LiTFSI, (b) Li_2S_8, (c) Li_2S_6, (d) Li_2S_4, (e) DOL, (f) DME and their binding energy.

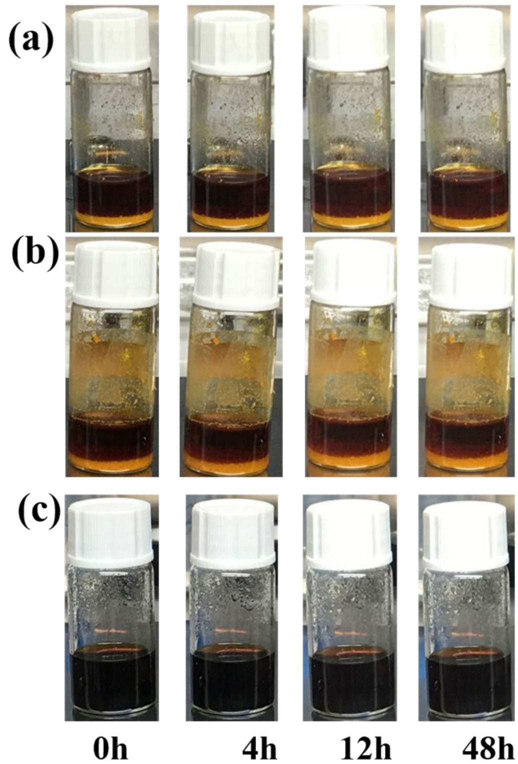

Figure S6. The photograph of the (a) Li_2S_6 , (b) Li_2S_6/LiTFIS solution after contacting with TPB-DMTP-COF. (c) The photograph of the Li_2S_6 solution after contacting with super-P.

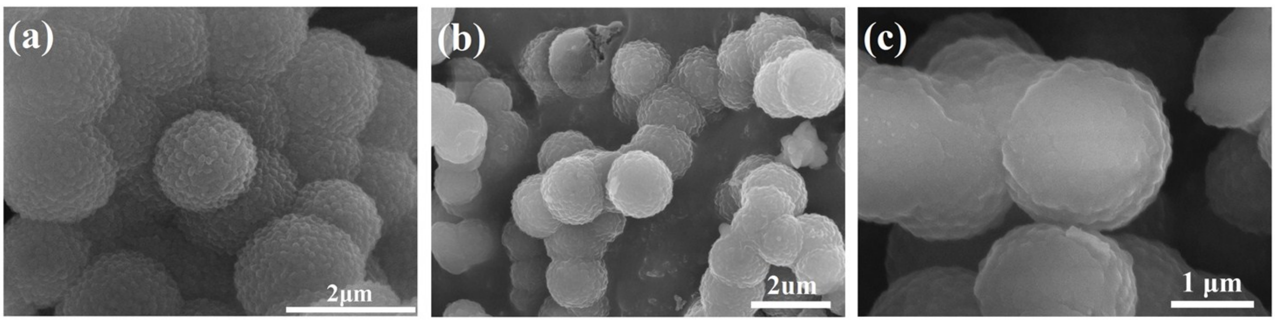

Figure S7. SEM of (a)TPB-DMTP-COF, (b)TPB-DMTP-COF/LiTFSI, (c)TPB-DMTP-COF/Li_2S_6.

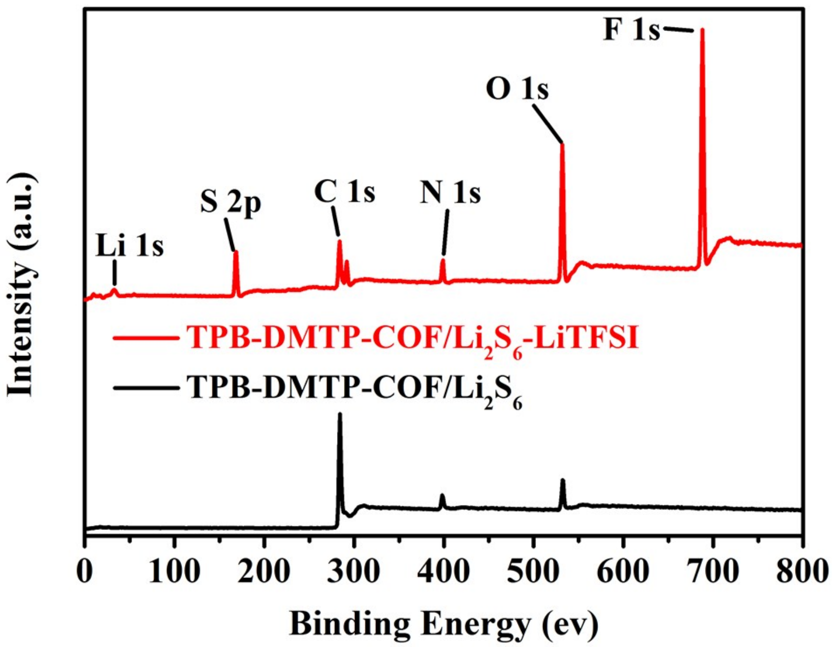

Figure S8. The XPS spectrum of COF after immersing in Li_2S_6 solution and Li_2S_6-LiTFSI solution.

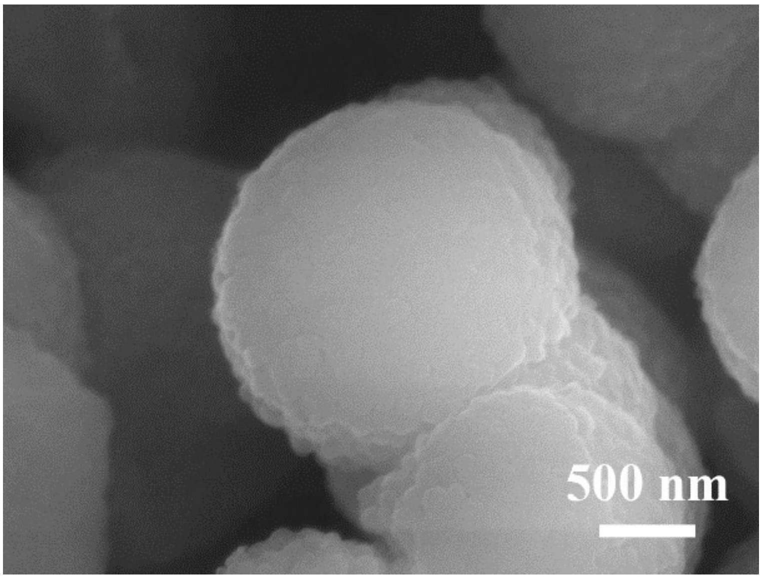

Figure S9. SEM of recovered TPB-DMTP-COF/LiTFSI.

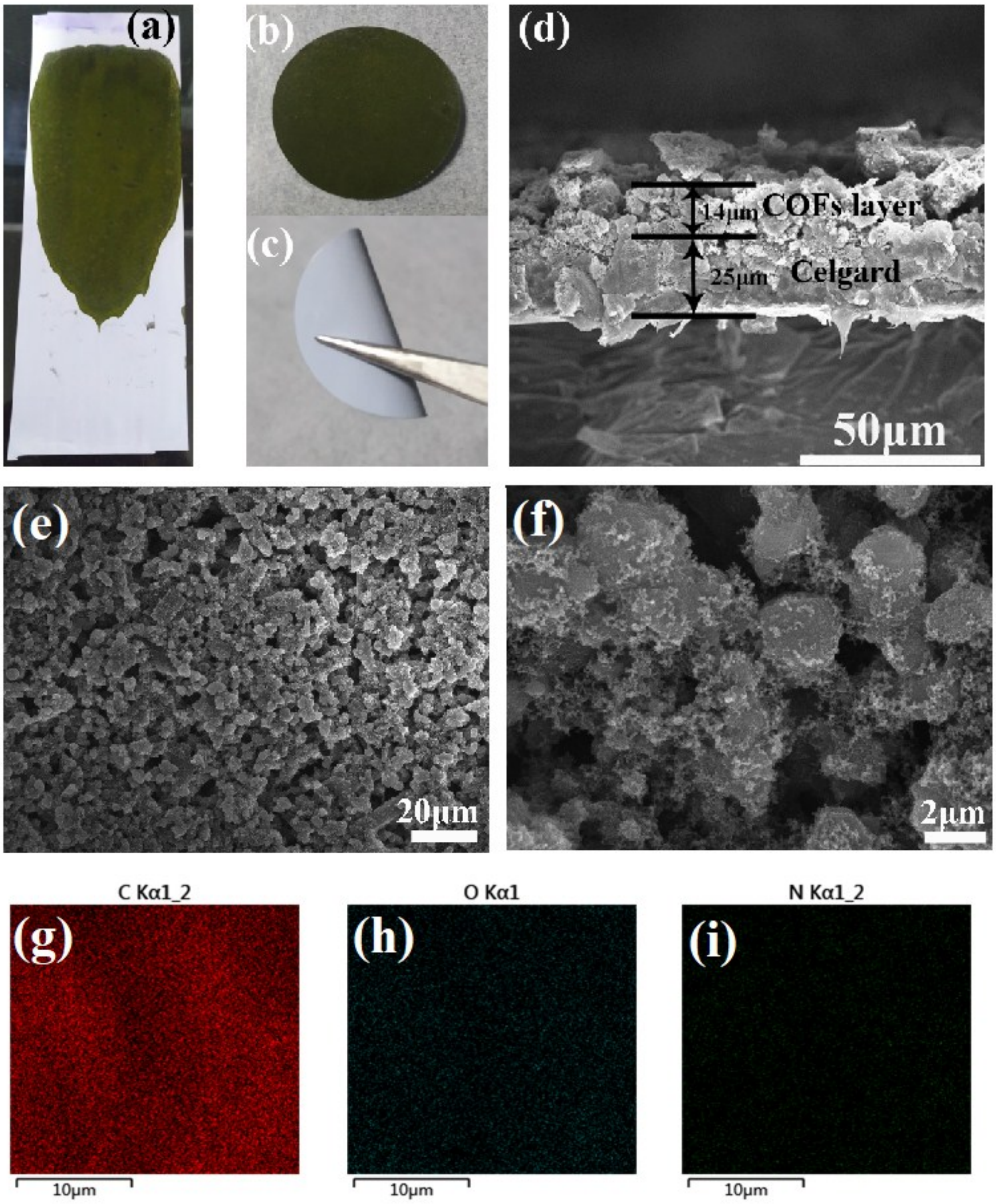

Figure S10. Digitabl images of the TPB-DMTP-COF coated Celgard separator (a, b, c). SEM images of the cross-sectional (d) and top surface (e, f) morphology of the TPB-DMTP-COF coated separator. (g-i) EDS mapping of the TPB-DMTP-COF coated Celgard separator.

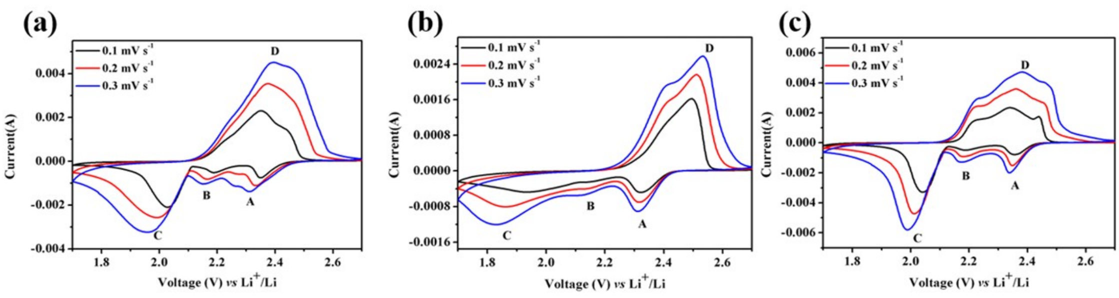

Figure S11. CV curves Li–SeS_2 cells with (a) super-P coating, (b) Celgard and (c) TPB-DMTP-COF coating at the scan rates of 0.1, 0.2 and 0.3 mV s^{-1}, respectively.

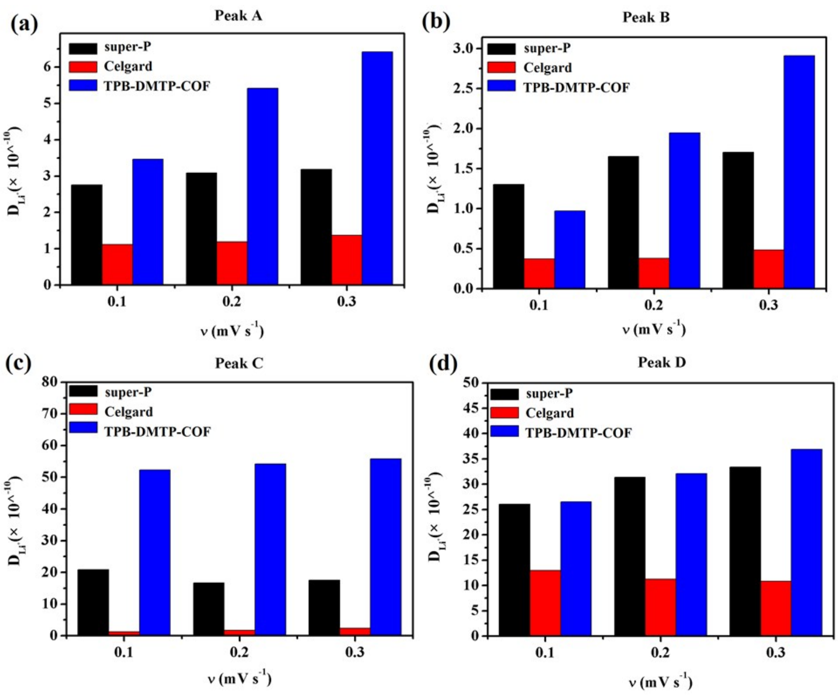

Figure S12. Comparison of lithium ion diffusion coefficient of the cells with different separator coating at different scan rates based on the peaks in CV plot with peak A (a) and peak B (b) (refers to SeS_2 →Li_2S_n and Li_2Se_n), peak C (c) (refers to Li_2S_n and Li_2Se_n → Li_2S and Li_2Se), and peak D (d) (Li_2S and Li_2Se → SeS_2).

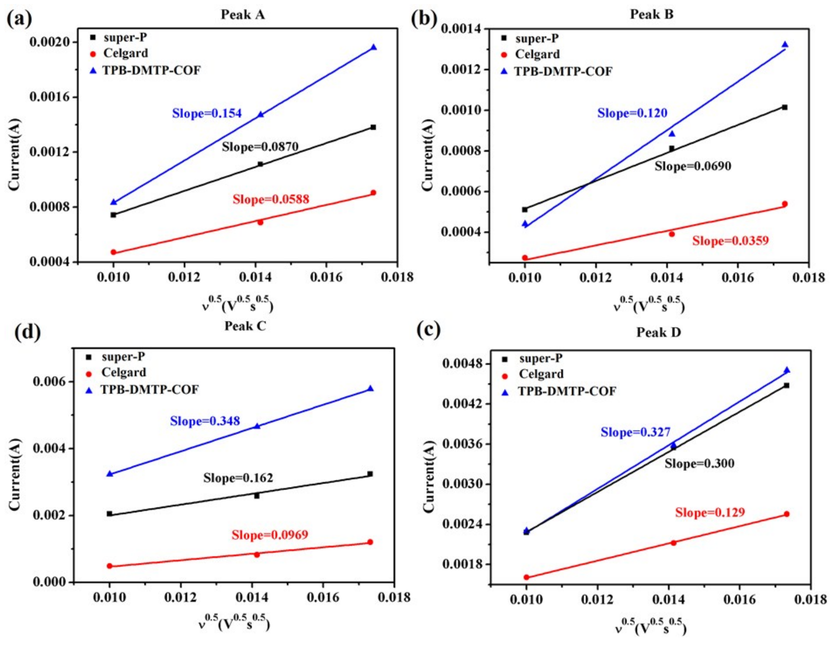

Figure S13. Plots of CV peak currents vs scan rate, (a) and (b) corresponds to the conversion of selenium disulfide to Li_2S_n and Li_2Se_n, respectively. (c) corresponds to the conversion of Li_2S_n and Li_2Se_n to Li_2S and Li_2Se.(d) corresponds to the conversion of Li_2S and Li_2Se to SeS_2

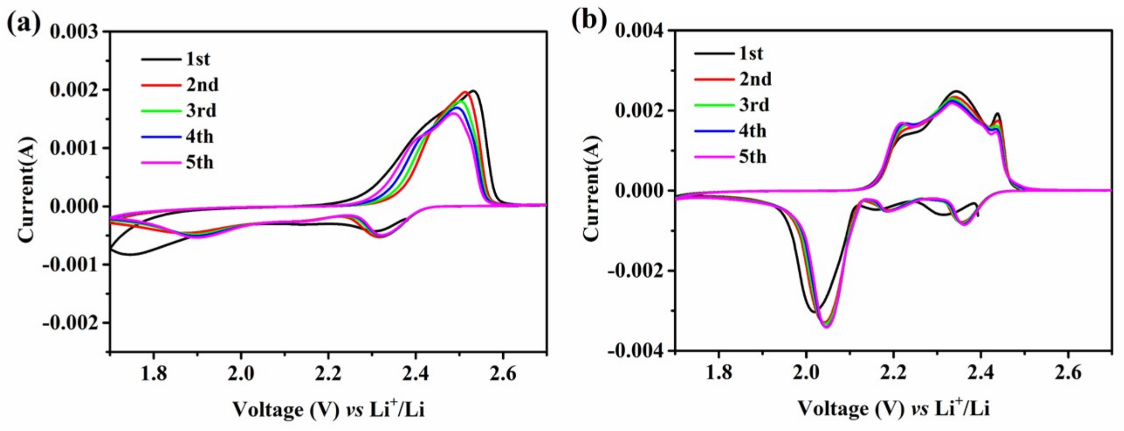

Figure S14. CV curves of the cell with (a) Celgard and super-P coated separator.

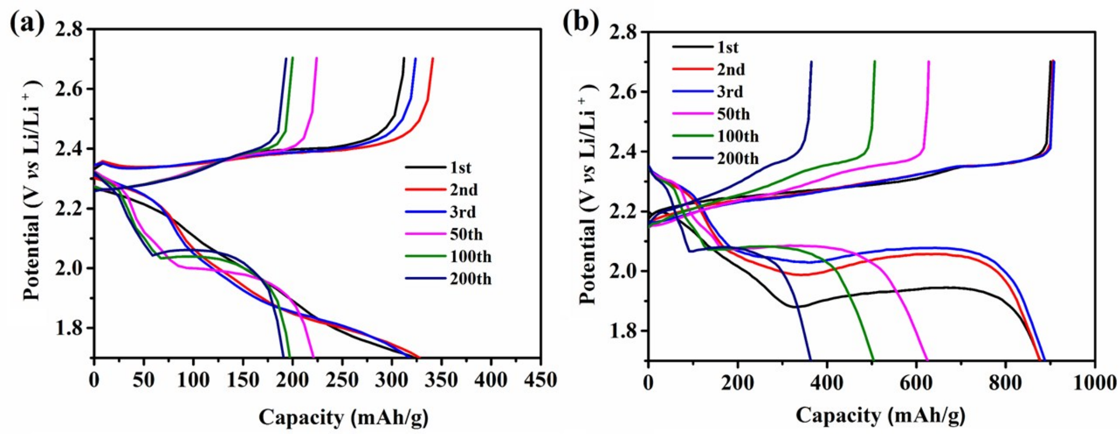

Figure S15. Galvanostatic discharge and charge profiles of the cell with (a) Celgard and (b) supre-P coated separator at 0.5 C.

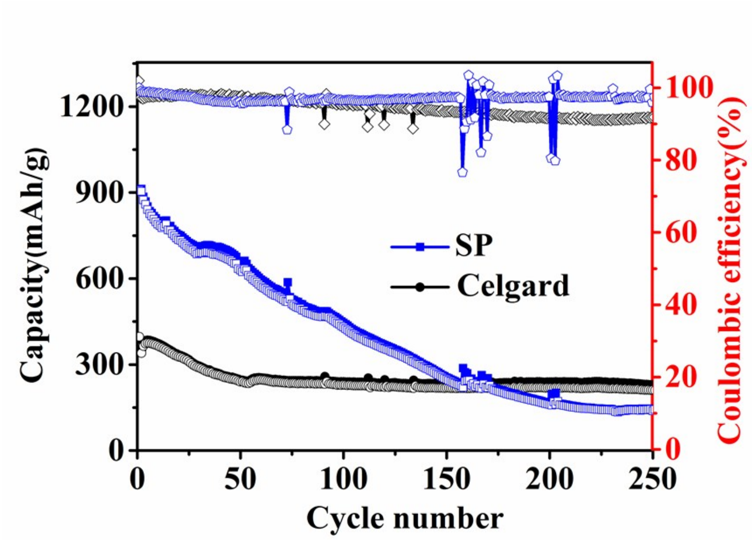

Figure S16. The cycling performance of Li-SeS_2 cell with Celgard or SP coated Celgard at 1 C (The SeS_2 loading is 4 mg/cm^2).

Reference

1. J. Zhang, Z. Li, X.W. Lou, Angew. Chem.Int. Ed. 2017, **56**, 14107-14112.
2. Z. Li, J. Zhang, H.B. Wu, X.W. Lou, *Adv. Energy Mater*. 2017, **7**, 1700281.

3. J. He, W. Lv, Y. Chen, J. Xiong, K. Wen, C. Xu, W. Zhang, Y. Li, W. Qin, W. He, *J.Mater.Chem.A* 2018, **6**, 10466-10473.
4. H. Zhang, L. Zhou, X. Huang, H. Song, C. Yu, *Nano Res*. **2016**, 9, 3725-3734.
5. C. Liu, X. Huang, J. Wang, H. Song, Y. Yang, Y. Liu, J. Li, L. Wang, C. Yu, Adv. Funct. Mater. 2018, **28**, 1705253.
6. Z. Li, J. Zhang, B.Y. Guan, X.W. Lou, *Angew. Chem. Int. Ed.* 2017**, 56**, 16003-16007.
7. Z. Zhang, S. Jiang, Y. Lai, J. Li, J. Song, J. Li, *J. Power Sources* 2015, **284**, 95-102.
8. P. Dong, K.S. Han, J.-I. Lee, X. Zhang, Y. Cha, M.-K. Song, *ACS Appl. Mater. Inter*. 2018, **10**, 29565-29573.
9. Z. Li, J. Zhang, Y. Lu, X.W. Lou, *Sci. Adv.* 2018, **4**, 1682-1687.